Archaeoastronomy and Ancient Technologies **2016**, 4(1), 1-18; http://aaatec.org/art/a_mg1

www.aaatec.org ***ISSN 2310-2144***

Theoretical Analysis of the Lunar Epicyclic Pin and Aperture System in the Antikythera Mechanism

Maria Giannopoulou

Independent researcher in collaboration with the University of Athens National and Kapodistrian University of Athens, Zografou, Attica, Greece;
E-Mail: mgianop222@gmail.com

Abstract

In this paper I develop a theoretical analysis of a two gear eccentric system in the Antikythera Mechanism, the oldest known analog computer. One gear carries a pin and as it rotates it transmits the motion to the other gear, which has an aperture. The angular velocity of the second gear depends from the shape of the aperture**.** Until now it was believed that the aperture was an orthogonal parallelogram. Prof. Xenophon Moussas expressed the idea that its shape could also be an ellipse or ellipse like. In this work the shapes *Slot*, *Ellipse* and *Parabola* are examined. The resulting motion of the gears is determined by a model in the framework of Lagrangian Mechanics. The theoretical results of the three shapes are compared with ephemeris data in order to specify which of them fits better with the data.

Keywords: Antikythera mechanism, ancient astronomy, ancient physics, prehistoric science, ancient technologies.

Introduction

The Antikythera Mechanism was discovered by Greek sponge divers in 1900 at the sea region of Antikythera island in Greece. Named after its place of discovery in a Roman shipwreck, it is technically more complex than any known device for at least a millennium afterwards [1]. It is the oldest computer and was produced probably in the second half of the 2nd century B.C. (between 150 and 100). It could make mathematical calculations by using gears made of bronze and estimate the positions of Sun and Moon relative with the stars and represents them to cyclic scales which show the zodiac, that is to say the sky with the stars (Fig.1) [2]. It also gives the date and probably the hour too. It displays the lunar phases and also keeps various calendars like the tropical which is still used for the agrarian works and lunar-sun calendars that the Greeks were using for their festivals, like the Olympic or the Nemea Games and nowadays for Easter. It can also predict the Sun and Lunar eclipses. Its dimensions were about 32×22×7 cm [2].

It is notable that the Antikythera Mechanism gives lunar motion by using a mechanism which emulate Kepler's 2nd law. That is to say the Moon moves faster when it is at the perigee and slower at the apogee. The exact definition of Luna's location in the sky is important because it can be used to calculate the geographical length [2].

In Figure 2a is represented a schematic sectional diagram of the gearing.

Figure 1. Reconstruction of the Antikythera mechanism in the National Archaeological Museum, Athens[1].

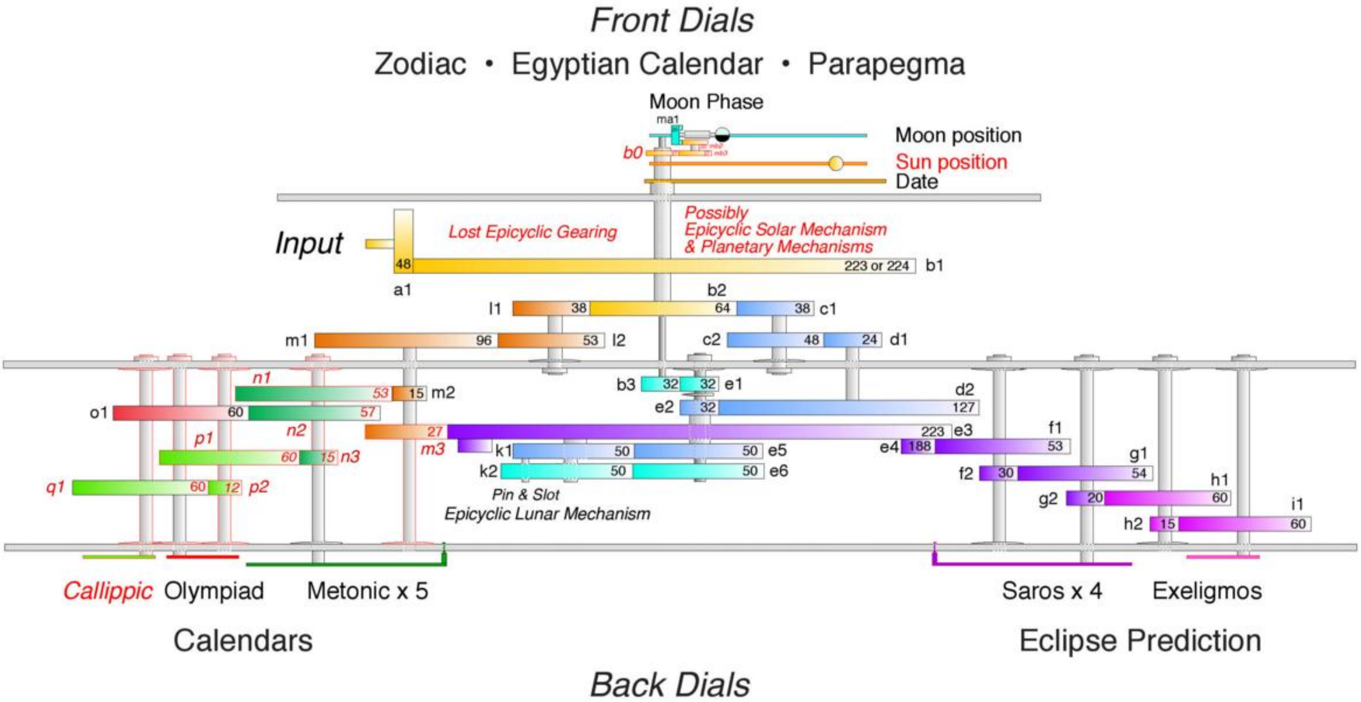

a

[1] https://archeocomputing.files.wordpress.com/2011/03/antikythera-mechanism2.jpg

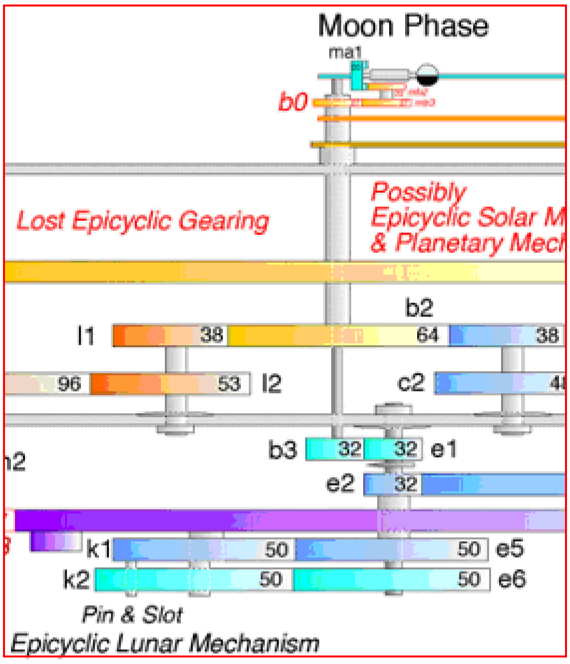

b

Figure 2. Antikythera mechanism**:** ***a*** **-** schematic sectional diagram of the gearing [3, Fig. 6], [4]; ***b*** **-** detailed view of Pin and Slot Hipparchos' lunar mechanism (gears k1, k2, e5, e6).

Figure 2b shows the gears that emulate Luna's motion. They are e5, e6, k1 and k2. As e5 rotates, it forces k1 which transmits the motion to k2 via a pin. Then k2 forces e6 to rotate. The gear k2 has an aperture and it's center is lightly offset from k1's center. The last two gears reproduce the differential lunar motion as seen from Earth. The result is displayed via e1 and b3 gears. Figure 3 shows the diagram of the lunar anomaly mechanism.

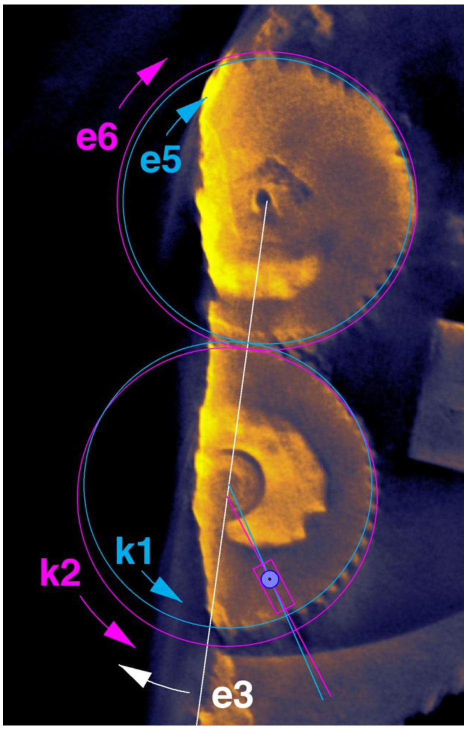

Figure 3. Diagram of the Lunar anomaly mechanism [3, Fig. 8], [5].

Prof. X. Moussas expressed the idea that the shape of the aperture might not be a parallelogram (slot- as drawn in Figure 3) but could also be an ellipse or ellipse like –maybe parabola, as shown in Figure 4.

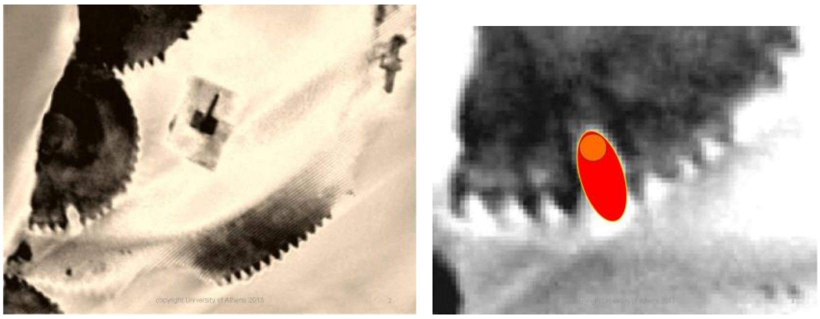

a ***b***

Figure 4. Lunar anomaly mechanism: ***a*** - CT slide, ***b*** - detailed view of ellipse by X. Moussas. [both pictures offered by X. Moussas[2]]

In the following theoretical analysis of the two-gear system k1 and k2, three different aperture shapes *Slot*, *Ellipse* and *Parabola* are examined in order to find out which of the three fits better to the ephemeris data.

Slot – Geometrical analysis

Let us consider two circles with the same radius r_o (Fig. 5)[3]. Let d be the distance between their centers O and O′ which is constant. So the length of the slot is 2*d*. The black circle represents the gear that carries the pin K, which moves in a circular path around O. Because the pin has dimensions we will from now on consider that point K is the center of the pin. (So r_o is the distance between the center of gear k1 and the center of the pin K.) Its angular velocity ω_o is constant. The vector $\overrightarrow{OK} = \vec{r}_o$ has also constant length r_o. The blue circle represents the gear that carries the slot. The center of the slot C, circuits around O′. It is obvious that the distance O′C is also r_o. We have $\overrightarrow{OO'} = \vec{d}$ so the radius $\vec{r} = \overrightarrow{O'K}$ is $\vec{r} = \vec{r}_o - \vec{d}$.

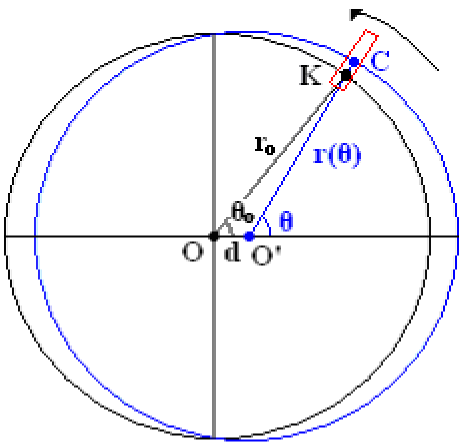

Figure 5. A schematic illustration of the gears with the relative offset of their centers.

[2] ©2013 Univercity of Athens
[3] Figures 5 – 22 are the author's copyright

So the length of $\vec{r}$ is $r(\theta)=\sqrt{r_o^2+d^2-2r_o d\cdot\cos\theta_o}$ and it depends from angle θ_o. We can estimate the angular velocity of K as seen from O′. We have:

$$\vec{r}_o = r_o\hat{r}_o \Rightarrow \dot{\vec{r}}_o = r_o\omega_o\hat{\theta}_o, \quad \theta_o=\omega_o t$$
$$\vec{r} = r\hat{r} \Rightarrow \dot{\vec{r}} = \dot{r}\hat{r}+r\omega\hat{\theta}, \quad \dot{\theta}=\omega$$

So

$$\vec{r}=\vec{r}_o-\vec{d} \Rightarrow \quad \dot{\vec{r}}=\dot{\vec{r}}_o \Rightarrow \quad \dot{\vec{r}}_o\cdot\dot{\vec{r}}_o=\dot{\vec{r}}\cdot\dot{\vec{r}}=\dot{r}^2+r^2\omega^2 \Rightarrow$$
$$(r_o\omega_o)^2=\frac{(r_o\omega_o d\cdot\sin\omega_o t)^2}{r_o^{\,2}+d^2-2r_o d\cdot\cos\omega_o t}+\left(r_o^2+d^2-2r_o d\cdot\cos\theta_o\right)\omega^2 \Rightarrow$$

$$\omega=\frac{\omega_o(1-z\cos\omega_o t)}{1+z^2-2z\cos\omega_o t}, \quad z\equiv\frac{d}{r_o}\ll 1$$

The blue gear carries the slot, which is parallel to O′C. So the gear rotates with ω, too. If we expand in Taylor series, we get:

$$\omega \simeq \omega_o+\omega_o z\cos\omega_o t+\omega_o z^2\cos 2\omega_o t+.... \quad (1)$$

A body that is being moved by a central force, generally follows a conic section. We are interested for an elliptical one. Let the focus (c, 0) be the tractive point and r_o the length of the semi-major axis. (Figure 6). In this case the body has a constant angular momentum $p_\theta=mr^2\dot{\theta}$. The angular velocity is then $\dot{\theta}=p_\theta/mr^2$.

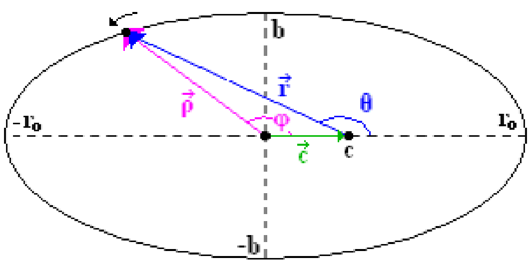

Figure 6. Motion in elliptical orbit.

We have $r=\dfrac{1-e^2}{1+e\cos\theta}r_o$ and $\dfrac{1}{r^2}=\dfrac{1}{r_o^2}+\left[\dfrac{2\cos\theta}{r_o^2}\right]_{e=0}e+\left[\dfrac{2+\cos^2\theta}{r_o^2}\right]_{e=0}e^2+.....$
where e is the orbits eccentricity.

For $e=0$, we take $\omega_o=\dfrac{p_\theta}{mr_o^{\,2}}=\dot{\theta}$ and $\theta=\omega_o t$, so we can write:

$$\dot{\theta}(t,\varepsilon)\simeq\omega_o+e2\omega_o\cos\omega_o t-e^2\omega_o\left(2+\cos^2\omega_o t\right)+... \quad (2)$$

The eccentricity of Moon's orbit is 0.0549 [6]. From Mechanism's measurements [7] we have:

$$z = \frac{d}{r_o} = \frac{1.1[mm]}{9.6[mm]} \simeq 0.114583 = 2 \times 0.0572917$$

That is to say that the relative offset of the two centers is estimated to be almost double than the eccentricity of Moon's orbit. Equations (1) and (2) coincide up to 1st order expansion.

Theoretical analysis of the two-gear system

Figure 7 represents an elliptical aperture and its positions as the gears rotate. The center of the Pin K moves along the half periphery of this ellipse, around C. Clockwise for $0<\theta<\pi$ and counterclockwise for $\pi<\theta<2\pi$. Mind that it's $r_o = 9.6[mm]$ and $d = 1.1[mm]$ [7].

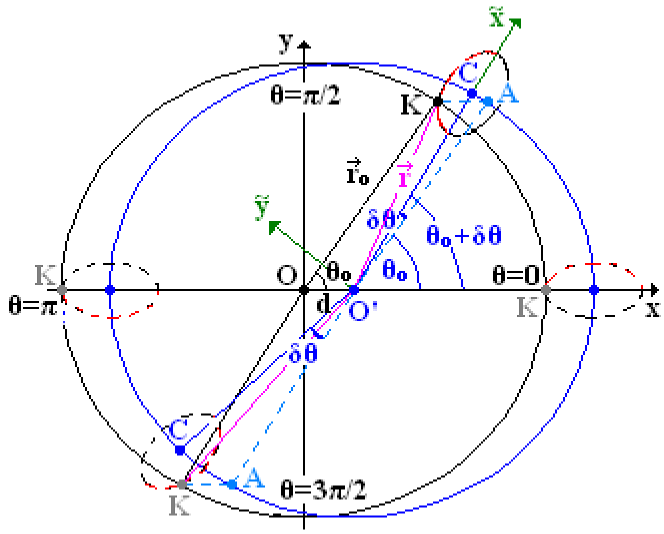

Figure 7. The positions of an elliptical aperture as the gears rotate.

We are referring to the Oxy Cartesian Coordinate System (CCS). We consider $\overrightarrow{KA} = \overrightarrow{OO'} \equiv \vec{d} = \begin{pmatrix} d \\ 0 \end{pmatrix}$ = constant vector. It is then $\overrightarrow{O'A} = \overrightarrow{OK} \Rightarrow \frac{d}{dt}\overrightarrow{O'A} = \frac{d}{dt}\overrightarrow{OK}$. So $\overrightarrow{O'A}$ forms an angle θ_o with the Ox semi axis and it moves with an ω_o angular velocity, as $\overrightarrow{OK}$. The angle between $\overrightarrow{O'C}$ and Ox semi axis, which we are interested for, is $\theta = \theta_o + \delta\theta$. It is obvious that $\delta\theta > 0$ at the upper semicircle and $\delta\theta < 0$ at the lower one. We also consider the rotating $O'\tilde{x}\tilde{y}$ CCS. As can be seen in Figure 7 the pin always moves on the half-plane with positive $\tilde{y}$. Since $\overrightarrow{O'C}$ is fixed on the blue gear, its angular velocity $\dot{\theta} = \omega_o + \delta\dot{\theta}$ is the one we are looking for. Note that for $\theta = 0$ it must be $\delta\dot{\theta} > 0$ and for $\theta = \pi$ it is $\delta\dot{\theta} < 0$. So we need to describe the motion as seen from the rotating $O'\tilde{x}\tilde{y}$ CCS.

The Lagrangian of the rotating pin K at the Oxy CCS (we denote as *m* it's mass) is:

$$L = \frac{1}{2}m\left(\dot{x}^2 + \dot{y}^2\right) - \frac{1}{2}m\omega_o^2\left(x^2 + y^2\right)$$

We are going to rewrite the Lagrangian to a more "compact" form. We set $q^1 \equiv x, \quad q^2 \equiv y$. We denote as n_{ij} the elements of the Euclidean metric, were $i, j = 1, 2$. We can use the dimensionless variables: $q^k \to q^k / r_o, \quad d \to d / r_o$, so becomes $|\vec{r}_o| = 1$.

We have then: $L = \frac{1}{2} m n_{ij} \dot{q}^i \dot{q}^j - \frac{1}{2} m \omega_o^2 n_{ij} q^i q^j$

We are going to rewrite the Lagrangian in terms of $\tilde{x}, \tilde{y}$ coordinates of the rotating system. The transformation is:

$$q^i = R^i{}_{\tilde{l}}(\theta)\tilde{q}^l + d^i \quad \text{where} \quad R^i{}_{\tilde{l}}(\theta) = \begin{pmatrix} \cos\theta & -\sin\theta \\ \sin\theta & \cos\theta \end{pmatrix}.$$

The new form of the Lagrangian is:

$$L = \frac{1}{2} m \tilde{n}_{kl} \dot{\tilde{q}}^k \dot{\tilde{q}}^l + \frac{1}{2} m \dot{\theta}^2 \tilde{n}_{kl} \tilde{q}^k \tilde{q}^l + m\dot{\theta} R\left(\frac{\pi}{2}\right)_{\tilde{l}\tilde{k}} \tilde{q}^k \dot{\tilde{q}}^l - \frac{1}{2} m \omega_o^2 \tilde{n}_{kl} \tilde{q}^k \tilde{q}^l - \frac{1}{2} m \omega_o^2 (d)^2 - m\omega_o^2 R^i{}_{\tilde{l}}(\theta) \tilde{q}^l d_i$$

Where $(d)^2 = \vec{d} \cdot \vec{d}$. The term $-m\omega_o^2 (d)^2 / 2$ may be omitted because it is constant and does not affect the equations of motion. We can also divide by the mass *m*, which is constant, too. We finally get:

$$L = \frac{1}{2} \tilde{n}_{kl} \dot{\tilde{q}}^k \dot{\tilde{q}}^l + \frac{1}{2} \dot{\theta}^2 \tilde{n}_{kl} \tilde{q}^k \tilde{q}^l + \dot{\theta} R\left(\frac{\pi}{2}\right)_{\tilde{l}\tilde{k}} \tilde{q}^k \dot{\tilde{q}}^l - \frac{1}{2} \omega_o^2 \tilde{n}_{kl} \tilde{q}^k \tilde{q}^l - \omega_o^2 R^i{}_{\tilde{l}}(\theta) \tilde{q}^l d_i$$

The equations of motion are $\frac{d}{dt}\left(\frac{\partial L}{\partial \dot{\tilde{q}}^s}\right) = \frac{\partial L}{\partial \tilde{q}^s}$. This leads us to:

$$\ddot{\tilde{q}}^r + \ddot{\theta} R\left(\frac{\pi}{2}\right)^{\tilde{r}}{}_{\tilde{k}} \tilde{q}^k + 2\dot{\theta} R\left(\frac{\pi}{2}\right)^{\tilde{r}}{}_{\tilde{k}} \dot{\tilde{q}}^k = \dot{\theta}^2 \tilde{q}^r - \omega_o^2 \tilde{q}^r - \omega_o^2 R(-\theta)^{\tilde{r}}{}_s d^s$$

We set *d* = 0.114583, *ωo* = 2*π* [*rad/sec*], and $\theta = \omega_o t + \delta\theta$ [*rad*]. The period becomes *T* = 1 [*sec*].

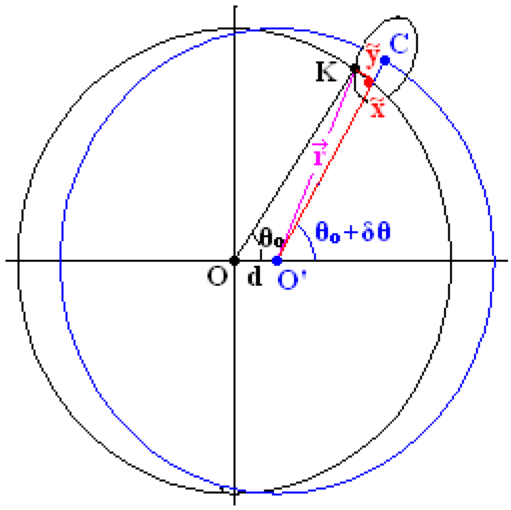

Figure 8. Coordinates of K $(\tilde{x}, \tilde{y})$ in the rotating $O'\tilde{x}\tilde{y}$ CCS.

The equations of motion are then:

$$\ddot{\tilde{x}}(t)-\tilde{y}(t)\delta\ddot{\theta}-\left(12.5664+2\delta\dot{\theta}\right)\dot{\tilde{y}}(t)-\tilde{x}(t)\left(12.5664+\delta\dot{\theta}\right)\delta\dot{\theta}+4.52357\cos\left(2\pi t+\delta\theta\right)=0$$
$$\ddot{\tilde{y}}(t)+\tilde{x}(t)\delta\ddot{\theta}+\left(12.5664+2\delta\dot{\theta}\right)\dot{\tilde{x}}(t)-\tilde{y}(t)\left(12.5664+\delta\dot{\theta}\right)\delta\dot{\theta}-4.52357\sin\left(2\pi t+\delta\theta\right)=0$$

For a given shape of the aperture with known parametric equations $\tilde{x}(t),\tilde{y}(t)$ (Figure 8), we finally take two differential equations of the unknown function $\delta\theta(t)$. We then solve the second equation for $\delta\ddot{\theta}$ and replace it at the first one, and we take a second order equation of $\delta\dot{\theta}$.

$$\begin{aligned}&-\delta\dot{\theta}^2\left[\tilde{x}^2(t)+\tilde{y}^2(t)\right]+\delta\dot{\theta}\left\{-12.5664\left[\tilde{x}^2(t)+\tilde{y}^2(t)\right]+2\dot{\tilde{x}}(t)\tilde{y}(t)-2\tilde{x}(t)\dot{\tilde{y}}(t)\right\}\\&\quad+4.52357\left[\tilde{x}(t)\cos\left(2\pi t+\delta\theta\right)-\tilde{y}(t)\sin\left(2\pi t+\delta\theta\right)\right]+12.5664\left(\dot{\tilde{x}}(t)\tilde{y}(t)-\tilde{x}(t)\dot{\tilde{y}}(t)\right)\\&\quad+\tilde{x}(t)\ddot{\tilde{x}}(t)+\tilde{y}(t)\ddot{\tilde{y}}(t)=0\end{aligned}$$

The algebraic solutions are two non-linear differential equations of first order $\delta\dot{\theta}_{1,2}=f_{1,2}\left(\tilde{x},\dot{\tilde{x}},\ddot{\tilde{x}},\tilde{y},\dot{\tilde{y}},\ddot{\tilde{y}},\delta\theta,t\right)$. One of them is going to be solved numerically.

For *Ellipse* the parametric equations verify the

$$\left(\tilde{x}-1\right)^2+\frac{\tilde{y}^2}{1-\varepsilon^2}=d^2.$$

where ε is the aperture's eccentricity.
It is also $\tilde{x}^2+\tilde{y}^2=r^2=1+d^2-2d\cdot\cos\omega_o t$.

From these two equations the accepted solution for $\tilde{x}(t)$ is:

$$\tilde{x}(t)=-\frac{\left(1-\varepsilon^2\right)}{\varepsilon^2}+\frac{1}{\varepsilon^2}\sqrt{1+d^2\varepsilon^4-2\varepsilon^2 d\cdot\cos\omega_o t}$$

The solutions for $\tilde{y}(t)$ are $\tilde{y}(t)=\pm\sqrt{1+d^2-2d\cdot\cos\omega_o t-\tilde{x}^2(t)}$,

but since we want $\tilde{y}\geq 0$ the corresponding equation is:

$$\tilde{y}(t)=\sqrt{1+d^2-2d\cdot\cos\omega_o t-\tilde{x}^2(t)}$$

As an estimate, based on Figure 4, the eccentricity of the elliptical aperture is about 0.98. We set semi-major axis d = 0.114583, ε = 0.98, ω_o = 2π [*rad/sec*] and we get the following graphs of Figure 9:

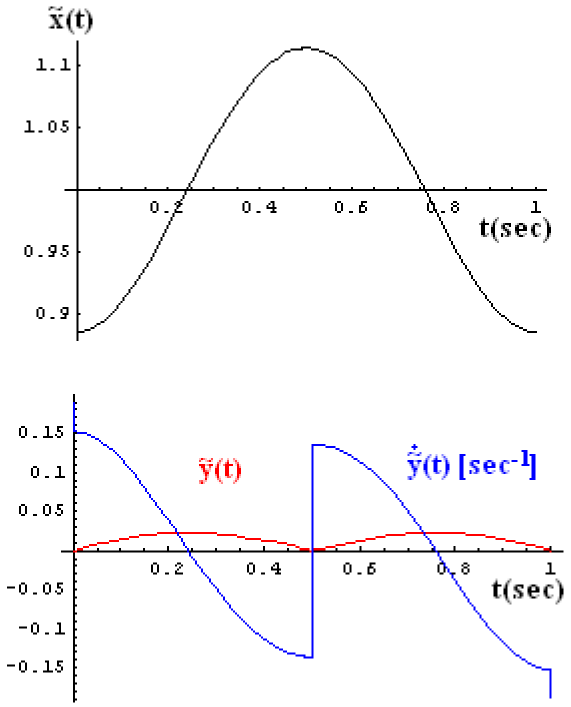

Figure 9. The parametric equations $\tilde{x}(t), \tilde{y}(t)$ and the time derivative $\dot{\tilde{y}}(t)$.

Equation $\tilde{x}(t)$ varies between $\tilde{x}(0)=0.885417$ (or 8.5 *mm*) and $\tilde{x}(0.5)=1.11458$ (or 10.7 *mm*). Equation $\tilde{y}(t)$ varies between $\tilde{y}(0)=0$ and $\tilde{y}(0.5)=0.0228018$ (or ~0.22 *mm*). The time derivative $\dot{\tilde{y}}(t)$ shows a gap at $t = kT/2$. This occurs when $\theta = k\pi,\quad k \in \mathbb{Z}$. From the parametric equations for initial conditions $t_o = 0.00001,\quad \delta\theta(t_o) = 0.00001$, we get $\delta\dot{\theta}_1(t_o) \simeq -13.551$ and $\delta\dot{\theta}_2(t_o) \simeq 0.641597$.

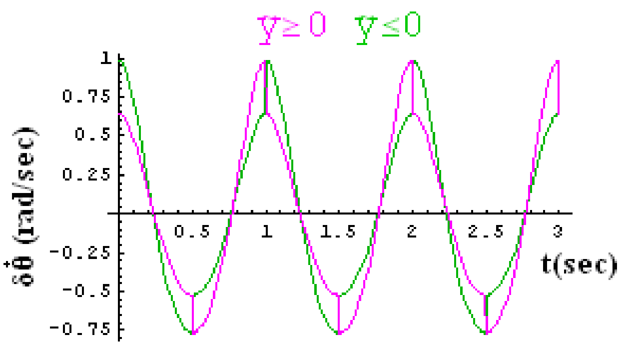

Figure 10. The modulation of the gear's angular velocity for the cases $\tilde{y} \geq 0$ and $\tilde{y} \leq 0$.

At $\theta = 0$ $\delta\dot{\theta}(t)$ is positive, so we are going to solve the second differential equation the $\delta\dot{\theta}_2 = f_2\left(\tilde{x}, \dot{\tilde{x}}, \ddot{\tilde{x}}, \tilde{y}, \dot{\tilde{y}}, \ddot{\tilde{y}}, \delta\theta_2, t\right)$. We find a numerical solution for $\delta\theta(t)$ and we plot the $\delta\dot{\theta}(t)$ at Figure 10. In the same Figure has been also plotted the case for which it would always be $\tilde{y} \leq 0$. The graph also shows a gap at $\theta = k\pi$, so *Ellipse* may not be a suitable shape for the aperture because it produces an intermitted movement of the gear.

Since we wanted to restrain the movement at the positive half axis, the Lagrangian should had been written as:

$$L=\frac{1}{2}\tilde{n}_{kl}\dot{\tilde{q}}^k\dot{\tilde{q}}^l+\frac{1}{2}\dot{\theta}^2\tilde{n}_{kl}\tilde{q}^k\tilde{q}^l+\dot{\theta}R\left(\frac{\pi}{2}\right)_{\tilde{l}\tilde{k}}\tilde{q}^k\dot{\tilde{q}}^l-\frac{1}{2}\omega_o^2\tilde{n}_{kl}\tilde{q}^k\tilde{q}^l-\omega_o^2\tilde{n}_{kl}\tilde{q}^k R(-\theta)^{\tilde{l}}{}_s d^s-c\Theta\left(-\tilde{q}^2\right)$$

There also should be a potential $-c\Theta(-\tilde{y})$ where c is a suitable positive constant. The corresponding equation of motion should then be:

$$\ddot{\tilde{y}}=4.52357\sin(2\pi t+\delta\theta)+\tilde{y}\left(12.5664+\delta\dot{\theta}\right)\delta\dot{\theta}-\left(12.5664+2\delta\dot{\theta}\right)\dot{\tilde{x}}-\tilde{x}\delta\ddot{\theta}+c\delta(\tilde{y})$$

There exists a force $c\delta(\tilde{y})$ that causes the reflection at point $\tilde{y}=0$. We tacitly assumed the existence of a potential $-c\Theta(-\tilde{y})$ when we selected the positive solution for $\tilde{y}$. The solution of the differential equation $\delta\dot{\theta}_2=f_2\left(\tilde{x},\dot{\tilde{x}},\ddot{\tilde{x}},\tilde{y},\dot{\tilde{y}},\ddot{\tilde{y}},\delta\theta_2,t\right)$ also shows a discontinuity.

Slot is a limit case of *Ellipse* with ε = 1 and parametric equations:

$$\begin{cases}\tilde{x}(t)=\sqrt{1+d^2-2d\cdot\cos\omega_o t}\\ \tilde{y}(t)\to 0\end{cases}$$

For initial conditions $t=0,\ \ \delta\theta(0)=0$, it is $\delta\dot{\theta}_1(0)\simeq-13.3774$ and $\delta\dot{\theta}_2(0)\simeq 0.811045$. So we will solve again the $\delta\dot{\theta}_2=f_2\left(\tilde{x},\dot{\tilde{x}},\ddot{\tilde{x}},\tilde{y},\dot{\tilde{y}},\ddot{\tilde{y}},\delta\theta_2,t\right)$. The solution is drawn in Figure 11 (blue) along with the *Ellipse*'s curves. In case of *Slot*, $\tilde{y}(t)=0$ is a continuous function. So the solution of $\delta\theta(t)$ is continuous as well.

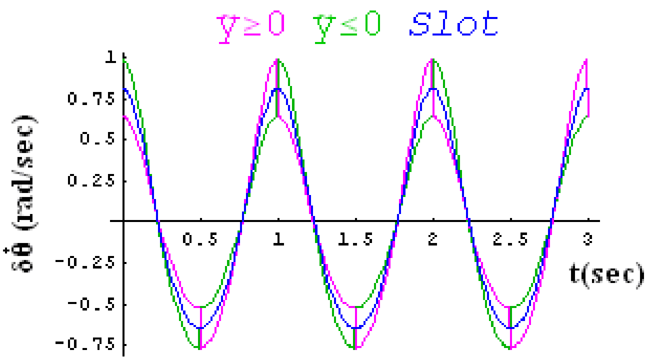

Figure 11. The modulation of the gear's angular velocity for *Ellipse* ($\tilde{y}\geq 0,\ \tilde{y}\leq 0$) and for *Slot* ($\tilde{y}=0$).

Let us examine now *Parabola*. We consider the same length of axes as in *Ellipse*. The parametric equations are:

$$\tilde{x} = 1 - d \cdot \cos\varphi(t)$$
$$\tilde{y} = d \cdot \sqrt{1-\varepsilon^2}\,\sin^2\varphi(t)$$

where $\varphi(t)$ is a nonlinear function of time. They lead us to the relation

$$\frac{(\tilde{x}-1)^2}{d^2} + \frac{\tilde{y}}{d \cdot \sqrt{1-\varepsilon^2}} = 1 \Leftrightarrow \quad \tilde{y} = d \cdot \sqrt{1-\varepsilon^2}\left[1 - \frac{(\tilde{x}-1)^2}{d^2}\right] \quad (3)$$

We have:

$$\left.\begin{aligned} \tilde{x}^2 + \tilde{y}^2 &= 1 + d^2 - 2d \cdot \cos\omega_o t \\ \tilde{y}^2 &= d^2\left(1-\varepsilon^2\right)\left[1 - \frac{(\tilde{x}-1)^2}{d^2}\right]^2 \end{aligned}\right\} \Rightarrow \quad \tilde{x}^2 + d^2\left(1-\varepsilon^2\right)\left[1 - \frac{(\tilde{x}-1)^2}{d^2}\right]^2 = 1 + d^2 - 2d \cdot \cos\omega_o t \quad (4)$$

The above equation (4) has four solutions. We call the one of interest $\tilde{x}_*(t)$. It shows a time delay of T/2 from the expected one. So our final result is $\tilde{x}(t) = \tilde{x}_*(t+0.5)$ and is drawn below. This also varies between 0.885417 (or 8.5 *mm*) and 1.11458 (or 10.7 *mm*) and the corresponding $\tilde{y}(t)$ oscillates between 0 and 0.0228018 (or 0.22 *mm*) as we expected.

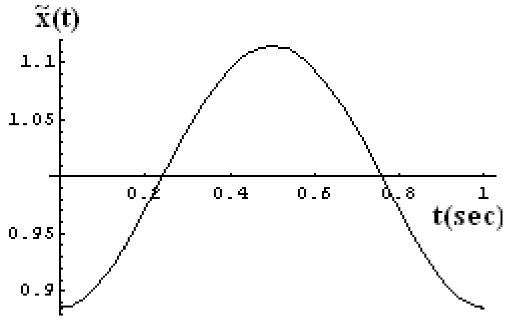

Figure 12. *Parabola*'s parametric equation $\tilde{x}(t)$.

The graph of the equation (3) is printed in Figure13.

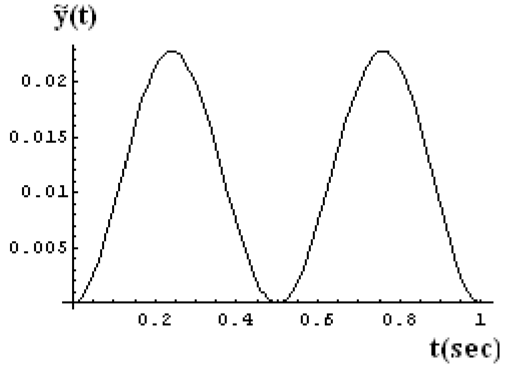

Figure 13. *Parabola*'s parametric equation $\tilde{y}(t)$.

Again, we have to solve the equation $\delta\dot{\theta}_2 = f_2\left(\tilde{x}, \dot{\tilde{x}}, \ddot{\tilde{x}}, \tilde{y}, \dot{\tilde{y}}, \ddot{\tilde{y}}, \delta\theta_2, t\right)$. Finally, we get a numerical solution for the angular velocity $\delta\dot{\theta}(t)$ which is shown below (Figure 14):

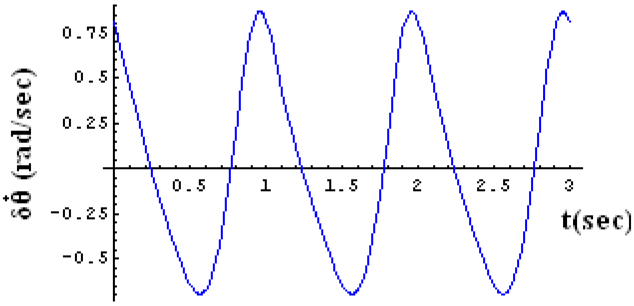

Figure 14. The modulation of the gear's angular velocity for *Parabola*.

Figure 15 shows a closed trajectory in the phase space. This means that we have a periodic curve, as we expected.

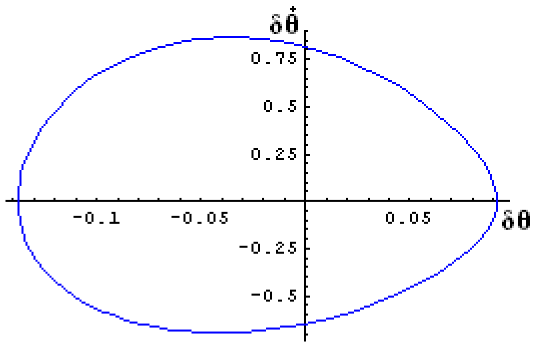

Figure 15. Closed trajectory in the phase space for *Parabola*.

The time derivative $\dot{\tilde{y}}(t)$ is continuous (Figure 16).

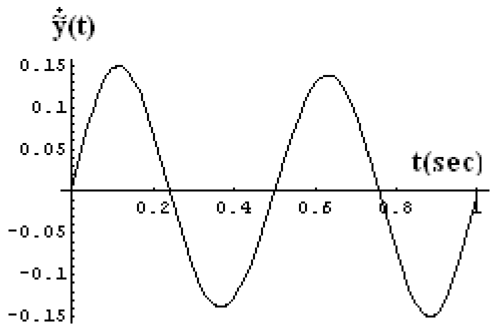

Figure 16. Time derivative $\dot{\tilde{y}}(t)$ for *Parabola*.

This is also confirmed by calculating the limits at points $t = 0$ and $t = 0.5$:

$$\dot{\tilde{y}}(0) = -3.9633 \cdot 10^{-17}, \quad \lim_{t\to 0^-} \dot{\tilde{y}}(0) = -3.9633 \cdot 10^{-17}, \quad \lim_{t\to 0^+} \dot{\tilde{y}}(0) = -3.9633 \cdot 10^{-17}$$

$$\dot{\tilde{y}}(0.5) = -6.29641 \cdot 10^{-17}, \quad \lim_{t\to 0.5^-} \dot{\tilde{y}}(0.5) = -6.29641 \cdot 10^{-17}, \quad \lim_{t\to 0.5^+} \dot{\tilde{y}}(0.5) = -6.29641 \cdot 10^{-17}.$$

Since the trajectory in phase space is closed, $\dot{\tilde{y}}(t)$ is continuous for every $\theta = k\pi, \quad k \in \mathbb{Z}$. The step function $c\Theta(-\tilde{y})$ is not needed to be present in Lagrangian's formula any more and this yields a continuous solution. The two shapes of the aperture are printed below (Figure 17):

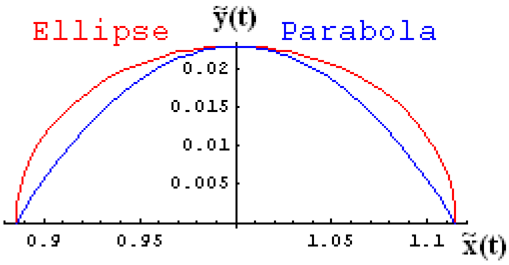

Figure 17. The shapes of an elliptical and a paraboloid aperture.

Note that the difference in the final results is due to the form of the shape, as can be seen in Figure 18 which shows the three cases synoptically.

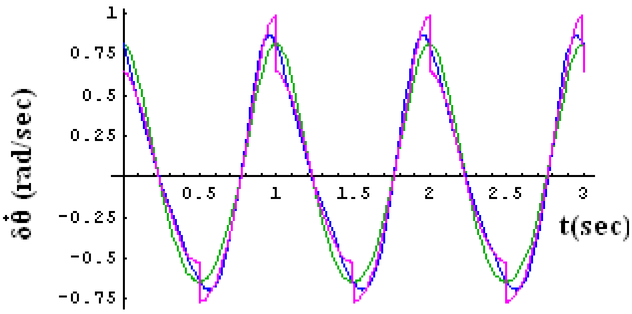

Figure 18. The modulation of the gear's angular velocity for *Slot* (green), for *Ellipse* ($\tilde{y} \geq 0$, violet) and for *Parabola* (blue).

Convert units to deg/day

The anomalistic period of the Moon is $T_{an} \simeq 27.55455$ [*days*][4] and the corresponding frequency is $\omega_{an} = \frac{360^o}{T_{an}} \simeq 13.065[deg/d]$ or $\omega_{an} = \frac{2\pi}{T_{an}} \simeq 0.228027[rad/d]$.

We said before that $\dot{\theta}(t) = \omega_o + \delta\dot{\theta}(\omega_o t)$ where we had set $\omega_o = 2\pi$ [*rad/sec*]. The expression of $\delta\dot{\theta}(\omega_o t)$ includes terms of $\cos\omega_o t$ where the argument is expressed in *rad*. We have to replace the angular velocity $\omega_o = 2\pi$ [*rad/sec*] by the anomalistic velocity $13.065[deg/d]$ and the period *T*=1 [*sec*] in $\delta\dot{\theta}(\omega_o t)$ by T_{an}. So we have:

$$\dot{\theta}(t) = 2\pi + \delta\dot{\theta}(2\pi t) \quad [rad/\sec] \rightarrow \quad \dot{\theta}\left(\frac{\deg}{day}\right) = 13.065 + \frac{13.065}{2\pi\left[\frac{rad}{\sec}\right]}\delta\dot{\theta}\left(2\pi\frac{t}{27.55455}\right)$$

The curves below can now be compared with the data:

---

[4] http://eclipse.gsfc.nasa.gov/SEsaros/SEsaros.html

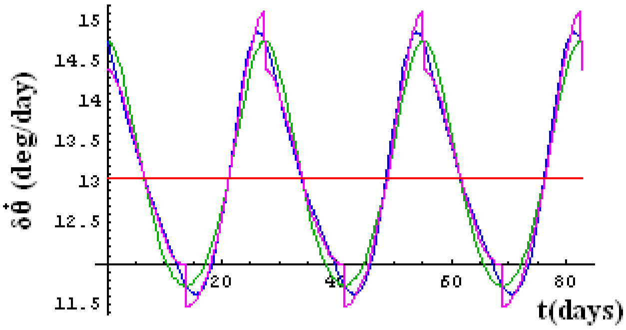

Figure 19. The modulation of the gear's angular velocity for *Slot* (green), for *Ellipse* ($\tilde{y} \geq 0$, violet) for *Parabola* (blue) and the anomalistic frequency (red).

Comparison with astronomical ephemeris data

The data cover the period from 1/1/2009 to 31/12/2013. The calculations were performed using an astronomical computer program HORIZONS System[5]. For each day we have the right ascension RA [*h*, *m*, *s*] and the declination δ [*deg*, *m*, *s*]. In order to compute the angular velocity we need to consider the celestial sphere (Fig. 20).

We also consider a spherical coordinate system where $\theta = \frac{RA[h]}{1[h]} 15$ [*deg*] and $\varphi = 90^o - \delta$ [*deg*] or $\theta = \frac{RA[h]}{1[h]} 15^o \frac{\pi[rad]}{180^o}$ [*rad*] and $\varphi = \frac{\pi}{2} - \delta^o \frac{\pi}{180^o}$ [*rad*].

The position vectors of the moon in Figure 20, are:

$$\vec{r}_1 = R(\sin\varphi_1 \cos\theta_1 \quad \sin\varphi_1 \sin\theta_1 \quad \cos\varphi_1)$$
$$\vec{r}_2 = R(\sin\varphi_2 \cos\theta_2 \quad \sin\varphi_2 \sin\theta_2 \quad \cos\varphi_2)$$

where R is the radius of the celestial sphere.

Let u be the angle between these two vectors. It is then:

$$\vec{r}_1 \cdot \vec{r}_2 = R^2 \cos u = R^2 \left[\cos\varphi_1 \cos\varphi_2 + \cos(\theta_1 - \theta_2)\sin\varphi_1 \sin\varphi_2\right] \Rightarrow$$
$$u = \arccos\left(\cos\varphi_1 \cos\varphi_2 + \cos(\theta_1 - \theta_2)\sin\varphi_1 \sin\varphi_2\right)$$

From the sourced data we can now calculate the angular velocity in *deg/day* or in *rad/day*.

We then compute the moving average of five terms: $\bar{u}_i = \frac{1}{5}\sum_{j=i-2}^{i+2} u_j$.

The results are represented in dots along with *Parabola*'s curve (blue) and Slot's curve (green) (Fig. 21). The computed mean values of minima and maxima of the ephemeris data are $\bar{\omega}_{\min} = 11.8883$ [*deg/d*] and $\bar{\omega}_{\max} = 14.689$ [*deg/d*]. They are shown in orange in Figures 21.

[5] http://ssd.jpl.nasa.gov/horizons.cgi#results

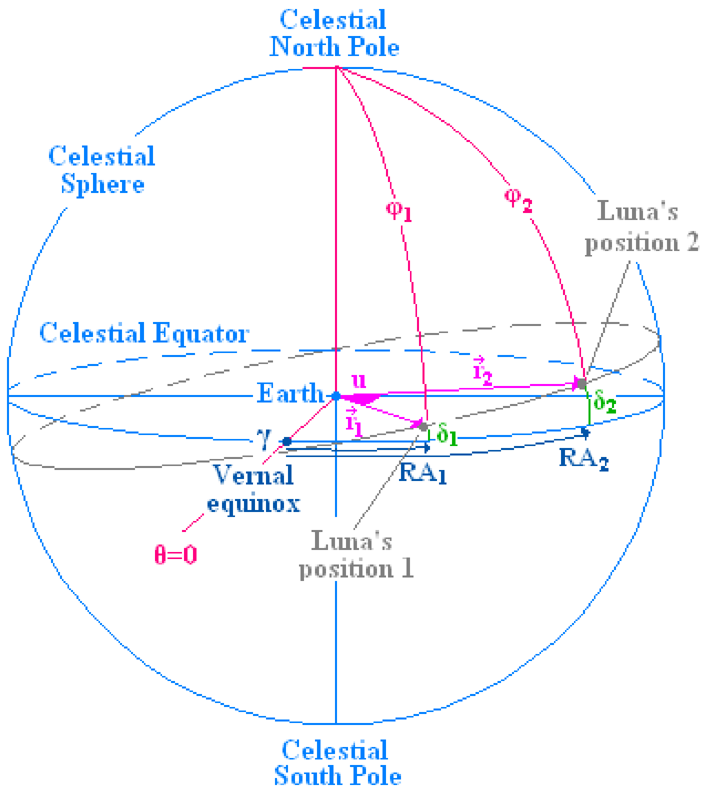

Figure 20. A schematic illustration of moon's trajectory in the Celestial Sphere.

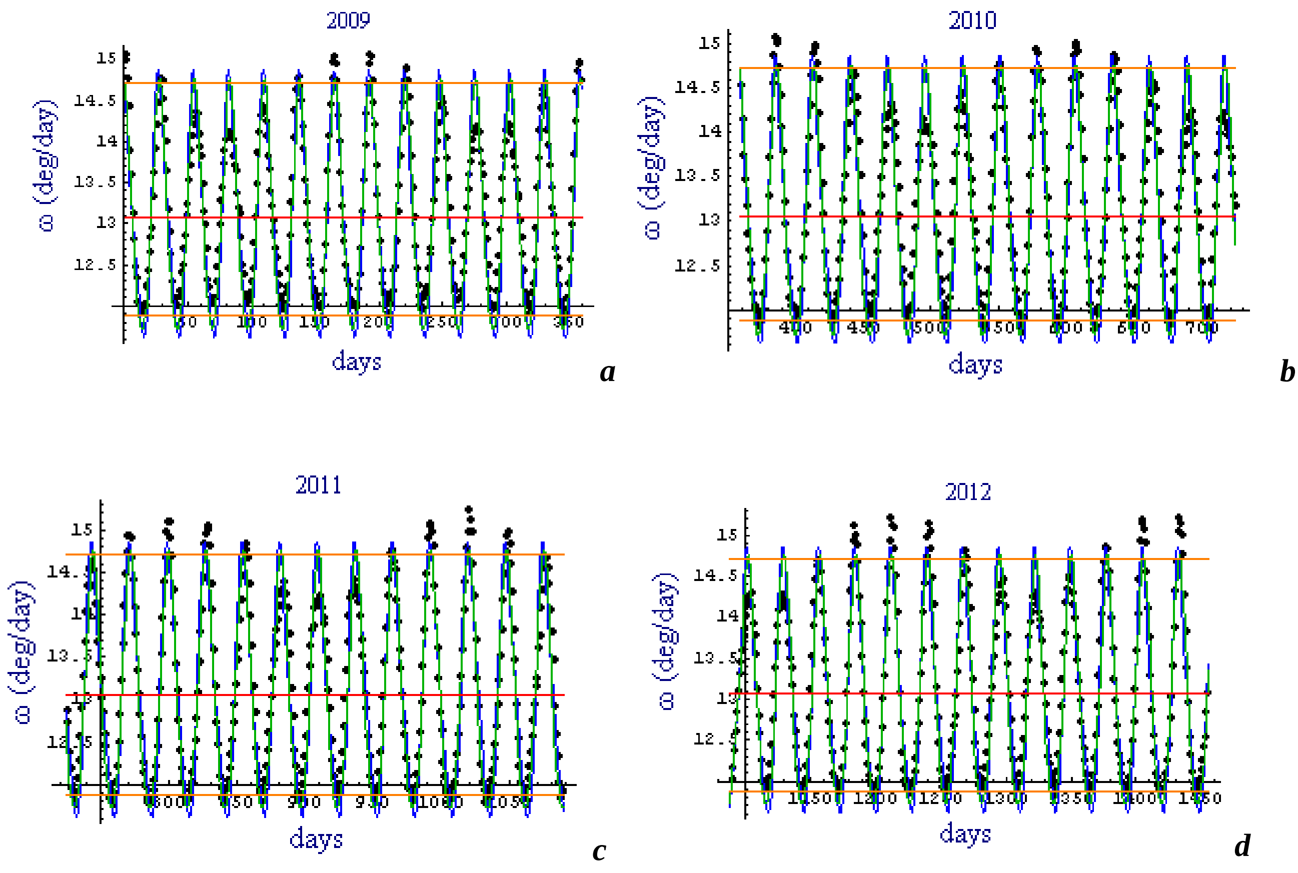

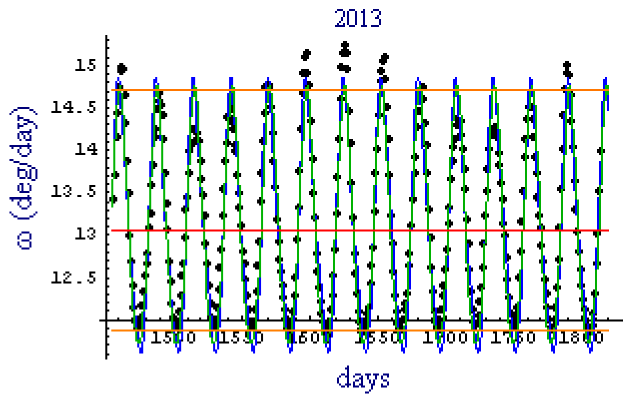

e

Figure 21. Comparison of the theoretical curves of *Slot* (green) and *Parabola* (blue) with the ephemeris data (dots), the anomalistic frequency (red) and the mean values of minima and maxima (orange). ***a*** - year 2009**,** ***b*** - year 2010**,** ***c*** - year 2011, ***d*** - year 2012**,** ***e*** - year 2013**.**

Now we are going to calculate the distribution of the deviation of the theoretical curves of *Slot* and *Parabola* from the computed moving averages:

$$dev_{Slot} = \frac{\bar{u}_i - \omega_{Slot}(t_i)}{\bar{u}_i}100, \quad dev_{Par} = \frac{\bar{u}_i - \omega_{Par}(t_i)}{\bar{u}_i}100$$

The statistics are:

Slot: Mean = 0.970374, Median = 1.3069 , Standard Deviation = 2.0113, Skewness = -0.664744

Parabola: Mean = 0.973558, Median = 1.13315, Standard Deviation = 2.54583, Skewness = -0.428225

Parabola's distribution shows a slightly larger standard deviation. The Histograms are given in below Figures 22a, b. In the above analysis of *Parabola* we assumed that the ratio of the minor semi axis (a) to the major semi axis (b) is $\sqrt{1-\varepsilon^2} \simeq 0.199$ which corresponds to $\varepsilon = 0.98$. If a = 1.1*mm* then b = 0.22*mm*. The question is which was the lower level of that age's micro-technology.

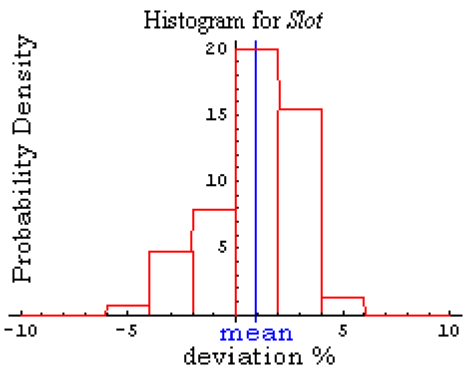

a

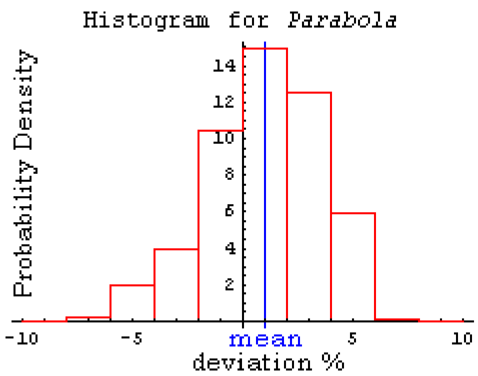

b

Figure 22. Histogram of the percent deviation of the theoretical curve from data**:** ***a*** **-** for *Slot*, ***b*** **-** for *Parabola*.

If we take into account that the pin has an unknown diameter then the major semi axis remains the same, since it is the distance between the center of gear k1 and the center of the pin K (as discussed earlier). But then the minor semi axis must be smaller. This means that the corresponding ε must be larger than 0.98. Furthermore, according to the geometrical analysis, since the eccentricity of moon's orbit is ~0.0549 [6], it should be *d* = 2×0.0549 = 0.1098.

For example, if we have $\varepsilon = 0.99$ and *d* = 0.1098, the statistics are:
Slot: Mean = 0.9442, Median = 1.0994, Standard Deviation = 1.8914, Skewness = -0.4178
Parabola: Mean = 0.9463, Median = 1.1076, Standard Deviation = 2.16, Skewness = -0.3664
The curves now seem to fit better with the data. The Mean and the Standard Deviation are smaller than the previous case. *Slot* still has a smaller standard deviation than *Parabola*.

The mean distances at perigee and apogee are 363300 [*Km*] and 405500 [*Km*] and the mean maximum and minimum orbital velocities are 1.076 [*Km/sec*] and 0.964 [*Km/sec*][6] respectively. We can compute the mean angular velocities at these points. They are $\omega_{\min} = 11.7685\left[deg/day\right]$ and $\omega_{\max} = 14.6617\left[deg/day\right]$. Remind that the computed minima and maxima of the data were $\bar{\omega}_{\min} = 11.8883^o/day$ and $\bar{\omega}_{\max} = 14.689^o/day$.

In the first case (where we had set ε = 0.98 and *d* = 0.114583) the minima and maxima of *Slot* and *Parabola* were

$$\omega_{\max,1}^{slot} = 14.7558^o/day,\ \omega_{\min,1}^{slot} = 11.7219^o/day,\ \omega_{\max,1}^{par} = 14.8627^o/day,\ \omega_{\min,1}^{par} = 11.6229^o/day$$

In the second case (ε = 0.99 and *d* = 0.1098) the minima and maxima of *Slot* and *Parabola* were

$$\omega_{\max,2}^{slot} = 14.6765^o/day,\ \omega_{\min,2}^{slot} = 11.7724^o/day,\ \omega_{\max,2}^{par} = 14.7307^o/day,\ \omega_{\min,2}^{par} = 11.7207^o/day$$

The ratios min/max are:

$$\frac{\omega_{\min}}{\omega_{\max}} = 0.803,\ \frac{\bar{\omega}_{\min}}{\bar{\omega}_{\max}} = 0.809,\ \frac{\omega_{\min,1}^{slot}}{\omega_{\max,1}^{slot}} = 0.794,\ \frac{\omega_{\min,1}^{par}}{\omega_{\max,1}^{par}} = 0.782,\ \frac{\omega_{\min,2}^{slot}}{\omega_{\max,2}^{slot}} = 0.802,\ \frac{\omega_{\min,2}^{par}}{\omega_{\max,2}^{par}} = 0.796$$

In both cases *Slot*'s value is closer to 0.803.

In the geometrical analysis for an elliptical orbit we had found: $r = \frac{1-e^2}{1+e\cos\theta} r_o$. If $r_{\min}$, $\dot{\theta}_{\max}$ are the distance and angular velocity at the perigee (where θ = 0) and $r_{\max}$, $\dot{\theta}_{\min}$ are the distance and angular velocity at the apogee (θ = π), due to angular momentum's conservation law it is $r_{\min}^2\dot{\theta}_{\max} = r_{\max}^2\dot{\theta}_{\min} \Rightarrow \dot{\theta}_{\min}/\dot{\theta}_{\max} = r_{\min}^2/r_{\max}^2$

So: $$\frac{r_{\min}}{r_{\max}} = \frac{1-e}{1+e} \Rightarrow \left(\frac{r_{\min}}{r_{\max}}\right)^2 = \left(\frac{1-e}{1+e}\right)^2 = 1-4e+8e^2-12e^3+.... \quad (5)$$

For *e* = 0.0549 it is $\left(\frac{r_{\min}}{r_{\max}}\right)^2 \simeq 0.803$.

The equation of *Slot* was $\omega = \frac{\omega_o\left(1-z\cos\theta_o\right)}{1+z^2-2z\cos\theta_o}$. So at points $\theta_o = 0$ and $\theta_o = \pi$, it is $\frac{\dot{\theta}_{\min}}{\dot{\theta}_{\max}} = \frac{1-z}{1+z}$.

For $z = 2e$, $$\frac{1-2e}{1+2e} = 1-4e+8e^2-16e^3+.... \quad (6)$$

For *e* = 0.0549, it is $\dot{\theta}_{\min}/\dot{\theta}_{\max} \simeq 0.802$.
Equations (5) and (6) coinside up to 2nd order expansion. *Slot*'s results are more accurate.

[6] http://nssdc.gsfc.nasa.gov/planetary/factsheet/moonfact.html

Conclusions

The above theoretical analysis illustrates the dynamics of the pin-aperture system. It is important to have an accurate measure of the eccentricity of Luna's orbit. The shape of the aperture introduces a potential which forces the gear to a differential rotation that simulates Lunar motion. The differences between the shapes are important especially at the minima and maxima The advantage of *Slot* is that it gives more accurate results and is easy to be manufactured. Other shapes with known parametric equations could also be examined in order to compare the produced motion with astronomical ephemeris data.

Acknowledgements

I wish to thank Prof. Xenophon Moussas for fruitful discussions and the provision of bibliography and photos.

References

1. Freeth, T.; Bitsakis, Y.; Moussas, X.; Seiradakis, J.H.; Tselikas, A.; Magkou, E.; Zafeiropoulou, M.; Hadland, R.; Bate, D.; Ramsey, A.; Allen, M.; Crawley, A.; Hockley, P.; Malzbender, T.; Gelb, D.; Ambrisco, W.; Edmunds, M.G. Decoding the ancient Greek astronomical calculator known as the Antikythera Mechanism. *Nature* 2006, 444, 587–591.
2. Moussas, X. *Antikythera Mechanism, PINAX (TABLET) the first computer and mechanical Cosmos* (in Greek), Ed. Hellenic Physical Union, Athens, Greece, 2011 and 2012 2nd edition.
3. Freeth, T.; Jones, A. The Cosmos in the Antikythera Mechanism, *ISAW* Papers 4, 2012. http://dlib.nyu.edu/awdl/isaw/isaw-papers/4/ (Access 05.02.2016)
4. Freeth, T.; Jones, A.; Steele, J. M.; Bitsakis, Y. Calendars with Olympiad display and eclipse prediction on the Antikythera Mechanism. *Nature* 2008, 454, 614-617 (partially available on http://www.nature.com/nature/journal/v454/n7204/extref/nature07130-s1.pdf).
5. Wright, M.T. The Antikythera Mechanism and the Early History of the Moon-Phase Display. *Antiquarian Horology* 2006, 29, 319-329.
6. Meeus, J. *Mathematical astronomy morsels.* Richmond, VA: Willmann-Bell, 1997; 11-12.
7. Gourtsoyannis, E. Hipparchus vs. Ptolemy and the Antikythera Mechanism: Pin–Slot device models lunar motions. *Advances in Space research* 2010, *46*, 540-544.